Hydrodynamics of the rupture of thin liquid films

By A. B. PANDIT and J. F. DAVIDSON

Department of Chemical Engineering, University of Cambridge, Pembroke Street,
Cambridge CB2 3RA, UK

Experiments on the rupture of a thin spherical liquid film – formed from a solution of surfactant – are reported. The mean film thickness, prior to rupture, was measured by an electrical conductivity method: initial film thicknesses were of order 0.3–0.9 μm. For an unruptured film, drainage due to gravity reduced the film thickness; the films ruptured naturally at a thickness of order 0.05–0.09 μm.

When the spherical film was punctured by a needle, a hole was formed, which grew rapidly, bounded by a liquid rim. As the rim moved, it collected the liquid from the film; but the rim was itself unstable, generating droplets continuously. The rim velocity, of order 10 m/s, was measured by cine photography at 2000 frames/s. Measured rim velocities compared well with a simple theoretical result derived from either (i) a force balance on the rim or (ii) an energy balance, which demonstrates that there is continuous energy dissipation due to collision between the moving rim and the elements of the stationary film.

When the moving rim had swept up the whole spherical film, much of the rim had disintegrated into droplets, but the remaining rim finally converged to give an 'implosion' generating more droplets. These droplets, together with those generated by fragmentation of the rim in flight, were collected: their number, of order 10^4, was measured by an image analyser, which also measured mean droplet size, of order 10^2 μm. The total droplet area was a few per cent of the area of the original spherical film.

1. Introduction

This paper describes experimental and theoretical work on the rupture of a thin liquid film when the film shatters to form droplets. It is common experience that the process of rupture is rapid: this can be observed by blowing a 'soap bubble', which is a thin liquid film, stabilized by surfactant and enclosing an almost spherical volume of air, typically 1–2 cm diameter. When the film is punctured, the bubble bursts rapidly, forming a number of droplets. The film rupture was described by Rayleigh (1891) who observed that when the film is partly ruptured, much of the liquid from the vanished film is concentrated into a rim which bounds the unbroken film, the rim breaking up as it moves, to form droplets. Rayleigh noted that the surface energy of the vanished film appears as kinetic energy of the rim; he quoted an estimated rim velocity of 16 yards a second, without giving details of his calculation or the formula from which the estimated velocity was obtained. Ranz (1959) described experiments to measure rim velocity, using an arrangement shown in figure 1. A flat soap film was formed, attached to what appears to have been a metal ring about 10 cm diameter; the film was then punctured by an electric spark in the middle of the ring. Subsequently, a moving liquid rim was photographed, the
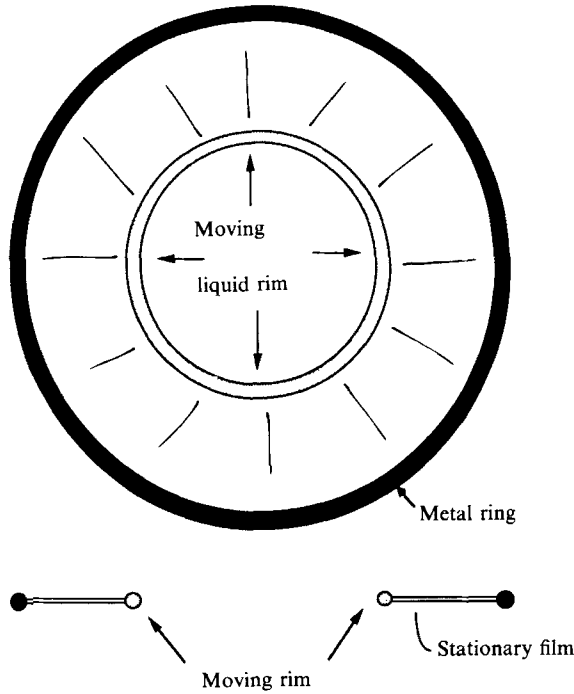
FIGURE 1. Rupture of flat soap film on a circular metal ring: the film is initially punctured at the centre of the metal ring (Ranz 1959).

rim being concentric with the containing ring: the moving liquid rim swept up the liquid film in its path, thus adding liquid to the rim. The rim appeared, from photographs, to have swept up all the liquid which had been in the area from which the film had vanished; but the rim evidently did not contain all the swept-up liquid, some having been lost, owing to the rim shedding droplets. Using the energy balance suggested by Rayleigh, Ranz obtained the following formula for the rim velocity:

$$v = (4\gamma/h\rho)^{\frac{1}{2}}, \tag{1}$$

where γ is the surface tension, ρ is the liquid density and h is the thickness of the original soap film. The energy balance shows that the rim velocity v is independent of the radius of the hole bounded by the rim: the progressively increasing surface energy liberated by rupture of the film appears as increased kinetic energy of the growing rim. Ranz showed that (1) was consistent with photographic measurements of rim velocity: the velocity was indeed independent of hole radius. He also measured the liquid film thickness and obtained fair agreement between observed rim velocity and (1): but the film thickness measurement involved measuring the very long focal length (7–10 m) of the soap film curved by gravity forces; this must have been difficult and prone to error.

Pandit, Philip & Davidson (1987) observed the rupture of the thin film of liquid formed when a rising bubble bursts through a horizontal liquid surface. They derived an equation like (1) but they used the force balance given by Taylor (1960) to predict the radius of the liquid sheet formed by two coaxial opposing jets; such a sheet is bounded by a stationary rim at a radius determined by the balance between (i) the inward forces of surface tension and (ii) the outward radial momentum of the liquid
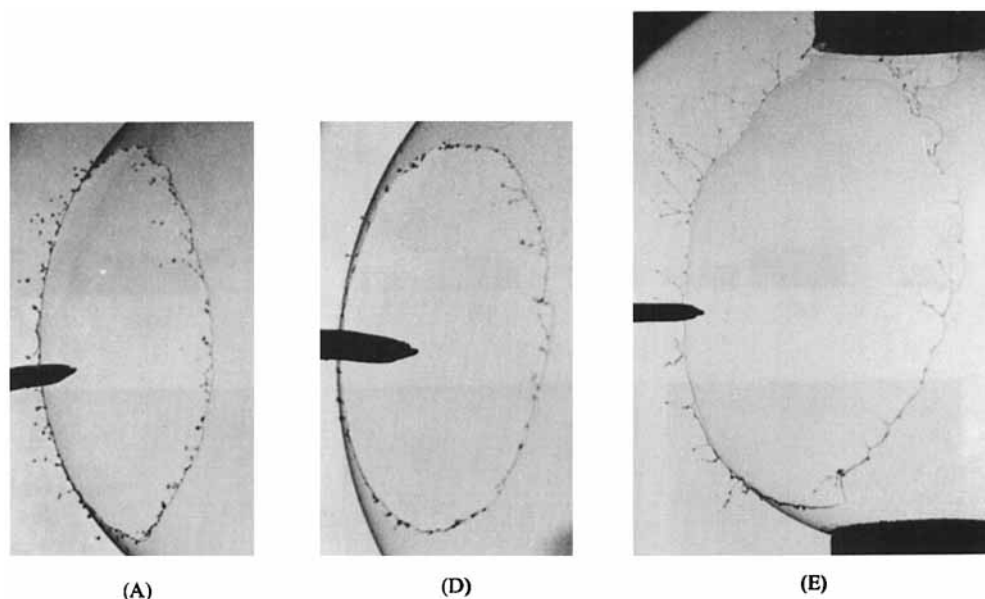
FIGURE 2. Close-up views of the rim moving round a spherical liquid film. Shedding of droplets from the rim is visible. (A), (D), and (E) show the effect increasing viscosity: the letters refer to table 1.

in the sheet. A liquid rim bounding a moving liquid sheet is familiar to those who study atomisers, e.g. Dombrowski & Fraser (1954).

The present paper describes work on the moving liquid rim, like that of Ranz (1959) which sweeps up the liquid from a thin stationary sheet as in the rupture of a soap bubble. Almost spherical soap films were used, so that the mean film thickness, prior to rupture, could be estimated from the conductivity between two electrodes in contact with opposite sides of the spherical film. The film was then punctured at one point by a needle, forming a 'rupture rim' of the kind described above, which swept up the spherical liquid film. Photographs of a typical rim are shown in figure 2. The rim velocity was measured by cine photography and the results were compared with theory using (i) a force–momentum balance like that of Taylor (1960) and (ii) an energy balance as proposed by Rayleigh (1891). The two methods give the same rim velocity, as they should; the energy balance reveals a continuous dissipation of energy, due to impact between the moving rim and the elements of the liquid film which are necessarily stationary until each element is subsumed by the moving rim. This energy loss was ignored by Ranz, so our prediction of rim velocity is $1/\sqrt{2}$ times the value given by (1).

The liquid rim breaks into droplets and there appear to be two mechanisms of breakage:

(i) The rim being approximately cylindrical, it is subject to the varicose instability, involving swellings and contractions, similar in character to that studied by Rayleigh (1945) and subsequently by many others (e.g. Rutland & Jameson 1971; Majumdar & Michael 1976). This leads to the shedding of droplets from the rim in flight, as seen in figure 2; the photographs are similar to those of Rayleigh (1891) and Ranz (1959).

(ii) In our experiments, the 'rupture rim' followed a nearly spherical path, as seen in figure 3, the rim shedding droplets as noted above. When the moving rim had
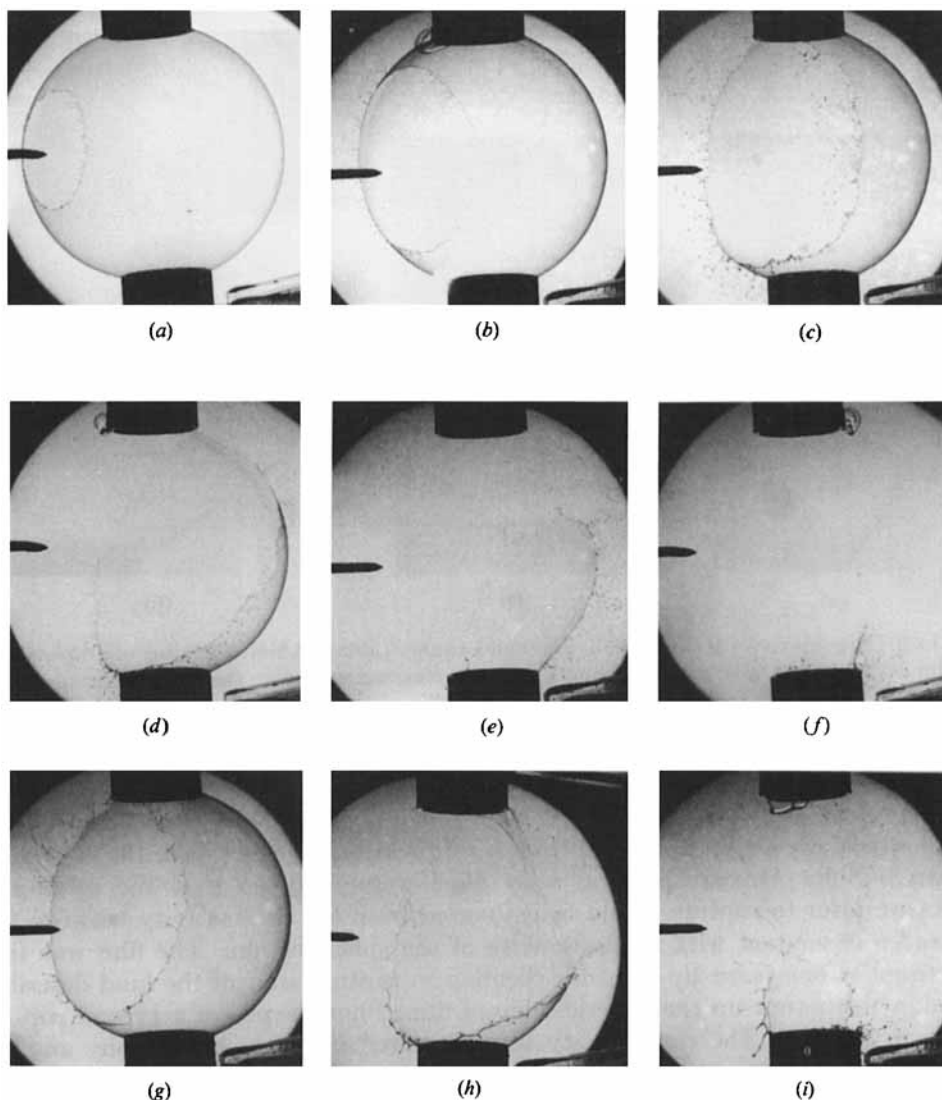
FIGURE 3. Flash photographs of liquid rim moving through a stationary spherical liquid film of diameter ≈ 50 mm and initial thickness ≈ 1 μm. Each photograph was from a separate experiment using the single flash equipment. Frames (a)–(f) are for aqueous Teepol solution, B table 1. Frames (g)–(i) are for glycerol, E table 1. The times after puncture of the film were (ms); (a) 2, (b) 5, (c) 7, (d) 9, (e) 12, (f) 13, (g) 7, (h) 9, (i) 12.

swept up all the liquid from the original soap film, it formed an 'implosion': elements of the rim from all parts of the original sphere converged in a region near to, but somewhat below, the point diametrically opposite to the original puncture of the spherical film; the final convergence of the elements of the film caused break-up into fine droplets. The fact that this final 'implosion' was at a lower level than the original puncture is believed to be due to thickening of the film in its lower regions due to gravity-induced drainage; the rim moves more slowly where the film is thicker and hence the asymmetry of the motion with respect to the diameter passing through the point of initial puncture.
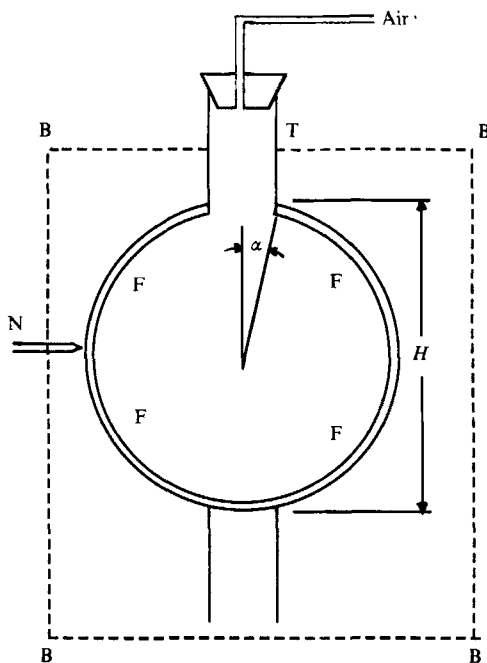
FIGURE 4. Apparatus for study of liquid film rupture. F is the spherical liquid film, held between two platinised metal tubes T (diameter 19.2 mm). The film is punctured by needle N. For collection of the droplets arising from film rupture, the film is surrounded by 'blotting paper' B.

Experiments, here described, were done to measure the number and size of droplets arising from both causes, i.e. from the rim instability, *en route*, and the 'implosion' which finally destroyed the rim.

The present work also included measurements of the 'critical film thickness' for the spherical soap film. The film was inflated, by the air supply shown in figure 4, to give an almost spherical shape: it was then allowed to drain until spontaneous rupture occurred at the critical thickness. The rim velocity experiments used film thicknesses much greater than the critical film thickness.

2. Experiments

2.1. *Formation of the bubble*

The apparatus is shown diagrammatically in figure 4. Two platinized metal tubes, of diameter 19.2 mm, were mounted with their axes vertical and coincident: the ends of the tubes were separated by a distance H, adjustable to within 0.1 mm.

The bubble was formed as follows. After wetting the end of each tube with the liquid, a beaker containing the liquid was placed so that the liquid surface contacted the bottom of the top tube: a thin liquid film, across the end of the tube, remained when the beaker was lowered. This horizontal film was then blown out by air supplied from the top tube: the blowing was stopped and the air supply tube pinched off, when the liquid film made contact with the top of the bottom tube. The bottom tube was sealed by that part of the liquid film which was within the diameter of the bottom tube, as shown in figure 4. The liquids used were: (i) aqueous solutions of Teepol and (ii) solutions of Teepol in glycerol. For each solution, the surface tension and electrical conductivity were measured. Properties are given in table 1.

Solution	Specific resistance (Ωm)	Surface tension (N/m)	Density ρ (kg/m³)	Viscosity μ (mPa s)
A	0.788	0.040	1004	2.0
B	0.666	0.035	1006	6.0
C	0.476	0.032	1008	10.0
D	2.43	0.028	1017	27.0
E	38.4	0.030	1060	260

TABLE 1. Physical properties of liquids used: A–D were aqueous solutions of Teepol; E was glycerol containing dissolved Teepol.

The bubble diameter was varied by varying H, the gap between the ends of the tubes, and H ranged from 20 to 80 mm.

2.2. Film thickness measurements

Using a potentiometer method, the apparent resistance R between the two tubes was measured. For a film of spherical form, the mean film thickness h was calculated from

$$h = \frac{\sigma}{2\pi R}\left[-\ln \tan^2\left(\tfrac{1}{2}\alpha\right)\right] \qquad (2)$$

obtained by integration of the potential gradients in the film due to the constant current therein. Here σ is the specific resistance of the liquid; α is the angle subtended by the ends of the tubes as shown in figure 4. A similar analysis can be made for any film profile connecting the two cylinders. For example, with a cylindrical film of radius $\tfrac{1}{2}H\tan\alpha$, $h = \sigma/\pi R\tan\alpha$.

The validity of the method was checked by rapidly deflating the film to minimize drainage. The deflation was continued until the film was cylindrical and of the same diameter as the tubes, 19.2 mm; the resistance between the tubes was then measured. The estimated total liquid volumes, calculated from (i) the spherical film thickness measurement using (2) and (ii) the cylindrical film thickness measurement, agreed well with one another.

The liquid film drained, owing to gravity. With a spherical film, the mean film thickness was measured as a function of time after the film was formed, up to the time t_c at which the film reached its critical thickness h_c, when it was inherently unstable and the bubble burst naturally.

2.3. Film rupture: rim velocity measurements

After measurements of the initial film thickness, as above, the film was punctured by the needle N, figure 4, which triggered the cine camera on making contact with the bubble. Taylor & Michael (1973) showed that a hole in a sheet of liquid will expand if the diameter of the hole is more than twice the thickness of the sheet. In the present work, the thickness of the liquid film was much less than the diameter of the needle point; consequently the hole created by the needle always expanded. The puncture was made immediately after formation of the bubble, so as to minimize film drainage prior to puncture. Early puncture was desirable, to get the thickest possible film and hence the slowest rim velocity, giving the maximum number of cine pictures during the rupture process.

After puncturing the film, the subsequent progress of the rupture process was

observed by cine photography at 2000 frames/s. Single flash equipment was used in separate experiments to get the photographs in figure 2 and figure 3: each photograph is from a separate spherical film. These single flash experiments were performed in total darkness, with the camera shutter opened just before the film rupture. A Nikon (FG20) 35 mm camera, equipped with a +2 close-up lens, was used. The single flash unit was activated by the electrical signal from needle N (figure 4), when it touched the liquid film; the electrical signal passed through a delay generator causing a controlled time delay of 1 to 30 ms between the needle touching the film and the light flash. Thus there was one flash at a predetermined time after the puncture. The single flash method was not suitable for velocity measurements, because each photograph was from a different spherical film. But rupture times deduced from the sequence of single flash photographs (as shown in figure 3) agreed well with results from the cine photographs.

The sequence of photographs from the cine film was like those in figure 3, but less sharp because the exposure time was necessarily longer than with the very short flashes for figure 3. The rim velocity was estimated from the cine pictures by two methods as follows:

(i) A mean rim velocity was obtained by measuring the time t_0 between (a) the puncture and (b) the rim implosion when the rim had just swept up the whole film: t_0 is the time for the rim to move round the whole periphery of the original sphere; it was obtained by counting frames and using the known framing rate.

(ii) Local values of rim velocity were obtained by measuring the distance travelled by the rim from one frame to the next.

2.4. *Mechanism of droplet formation*

The mechanism of droplet formation can be seen from figures 2 and 3, especially 3 (*g*) and 3 (*h*), showing behaviour with liquid of high viscosity: evidently the moving rim forms jets of liquid and each jet becomes unstable to form droplets. The breakup of the rim can be seen in figure 2, which is a close up view of the rim, showing the breakup into jets from which droplets are subsequently formed. It is evident that when the viscosity increases, the jets are further apart and have increased length prior to breakup. Larger and fewer droplets are therefore formed as the viscosity increases.

2.5. *Number and sizes of droplets generated*

To observe the number and sizes of droplets generated, the spherical soap bubble was surrounded by a complete cylinder of porous paper, BBBB (figure 4), like blotting paper. A dye – India ink for the aqueous solutions and for the glycerol – was added to the liquid forming the bubble. The blotting paper collected virtually all the droplets formed from the rim by the shedding in flight and from the final implosion of the rim. The sizes of the ink blots formed on the blotting paper had been calibrated with respect to the droplets from which they were formed.

The large number of 'ink blots' on the blotting paper was examined by an image analyser, which gave the number of droplets, their mean size and the standard deviation of the size distribution.

3. Theory

3.1. *Momentum balance*

Figure 5 shows the forces on an element of liquid rim. The rim was formed by picking up all elements of the thin flat film originally within the radius r and angle $d\theta$. The
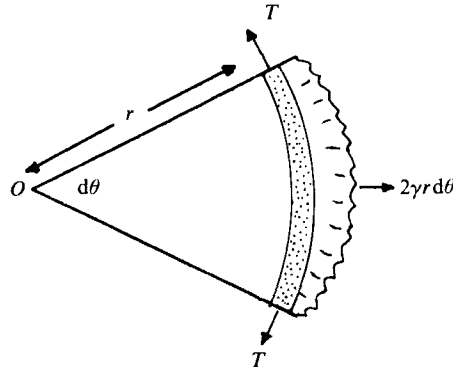
FIGURE 5. Forces on an element of rim, the rim formed from the vanished flat film between
O and radius r.

forces on the rim are due to surface tension and must equate with the change of radial
momentum of the rim. This method of analysis is essentially similar to that of Taylor
(1960) who considered a stationary rim bounding a thin liquid sheet generated by
two opposed coaxial jets.

It is readily shown that the radial component of the tangential forces T is
negligible in comparison with the radial force $2\gamma r\,d\theta$; the radial and tangential forces
are due to surface tension. Hence, from a momentum balance,

$$\frac{d}{dt}(\rho A r\,d\theta\,v) = 2\gamma r\,d\theta, \tag{3}$$

where A is the cross-sectional area of the rim. It is assumed that the rim contains all
the liquid originally in the thin film of radius r and thickness h, so that from
continuity, $Ar\,d\theta = \frac{1}{2}r^2 h\,d\theta$, and combining this with (3) gives

$$\rho h \frac{d}{dt}\left(\tfrac{1}{2}r^2 \frac{dr}{dt}\right) = 2\gamma r. \tag{4}$$

A solution to this equation of motion is $v = dr/dt = $ constant, giving

$$v = (2\gamma/\rho h)^{\frac{1}{2}}. \tag{5}$$

Now (4) is a second-order differential equation and there may be other solutions
besides (5); this question will be discussed below. A similar derivation was given by
Pandit *et al.* (1987) but an incorrect use of the continuity equation led to a different
numerical coefficient within the square root in (5).

3.2. *Energy balance*

As noted above, Ranz (1959) used an energy balance to derive (1). But he ignored the
energy dissipation due to collision of the moving rim with elements of the stationary
film. Using a momentum balance, it is readily shown that when liquid of mass M,
moving with velocity v, amalgamates with a small liquid element of mass dM, the lost
energy is $\frac{1}{2}dMv^2$. Now consider a moving rim, as in figure 5, formed from a vanished
film of area A_f; the film may be flat, spherical, or of other shape. The energy balance
is then

$$2\gamma dA_f = d(\tfrac{1}{2}Mv^2) + \tfrac{1}{2}v^2\,dM, \tag{6}$$

where M now denotes the mass of the rim. On the right-hand side of (6), the first term

represents the change of rim energy and the second is the energy dissipation due to impact of the rim with elements of the film. In formulating (6), the surface energy of the rim, being small, was ignored. This is equivalent to neglecting the radial component of the forces T in figure 5. Order of magnitude calculations show that the surface energy of the rim is 2–3 % of the surface energy of the original film. From continuity, $M = \rho A_f h$ which with (6) gives

$$4\gamma M = \rho h \frac{\mathrm{d}}{\mathrm{d}M}(M^2 v^2). \tag{7}$$

Provided the centre of the rim moves along the centreline of the film, (7) is valid for all shapes of film. For a curved film – as in the present experiments – the path of the rim may deviate from the centreline of the film owing to centrifugal forces; this will be discussed below in §3.4.

Equation (7), and consequently (5), are valid for a 'linear rim' arising when a flat film of liquid is punctured along a straight line. It applies also for a point puncture, generating an expanding circular rim as in figure 1. In this case it may readily be shown that (4) and (7) are equivalent, as follows. Referring to the right-hand side of (7),

$$\mathrm{d}(M^2 v^2)/\mathrm{d}M = 2Mv^2 + 2M^2 v\,\mathrm{d}v/\mathrm{d}M.$$

Putting $M = \rho \pi r^2 h$ and $\mathrm{d}M = 2\pi \rho r h v\,\mathrm{d}t$, (7) then becomes

$$2\gamma r = \rho h(rv^2 + \tfrac{1}{2}r^2\mathrm{d}v/\mathrm{d}t),$$

which is the same as (4). Hence (7) is merely a restatement of (4) with the advantage that it can be integrated to give

$$M^2 v^2 = 2\gamma M^2/\rho h + C,$$

where C is an integration constant. It follows that

$$v^2 = (2\gamma/\rho h) + C/M^2. \tag{8}$$

The first term on the right-hand side of (8) leads to (5). The second term depends upon the initial conditions. If $v = 0$ when $M = 0$, as in the present experiments, the film starting from rest, then $C = 0$ so that (8) and (5) are identical. If C is finite, as for example when the rim received an initial impulse, then (8) tends to (5) when M is large so that (5) represents the asymptotic velocity of a rim sweeping up a thin liquid film.

The energy balance is thus a useful alternative method of deriving the equation of motion of the rim, particularly as it gives a readily integrable form, (7). There is additional utility in the energy balance when breakup of the rim into droplets is considered. If the velocity of the droplets arising from the rim is the same as that of the rim, and if the surface energy of the droplets is small, then the energy balance (7) will not be affected by rim breakup.

A final point with regard to the energy balance is that it was used in deriving (1), but ignoring the energy dissipation due to impact between the moving rim and the stationary film: thus (5) predicts a velocity $1/\sqrt{2}$ times (1); this effect of energy dissipation was noted by Culick (1960), who derived (5) by using a combination of the momentum and energy balance methods.

3.3. *Fixed rim, moving film: energy dissipation*

Having established, as above, that there is constant rim velocity when the rim grows by sweeping up a fixed liquid film, it is helpful to consider a frame of reference moving with the rim: this is the case considered by Taylor (1960); the flowing film feeds liquid steadily into the fixed rim. A momentum balance per unit length of rim then equates (i) the rate of momentum flux $\rho v^2 h$ with (ii) the surface tension force 2γ, giving (5). The entire kinetic energy of the film is lost, so the rate of energy dissipation, per unit length of rim, is $\frac{1}{2}\rho v^3 h$. This may be compared with the result from the analysis of §3.2 for a stationary film swept up by a moving rim. From the derivation leading to (6), the rate of energy dissipation is $\frac{1}{2}v^2 \mathrm{d}M/\mathrm{d}t = \frac{1}{2}\rho v^3 h$, using $\mathrm{d}M/\mathrm{d}t = \rho v h$, i.e. the same energy dissipation rate as from 'the fixed' rim analysis. With the moving rim, the rate of loss of surface energy by the swept-up film is $2v\gamma = \rho v^3 h$, using (5). Half of this energy is converted into the kinetic energy of the moving rim $\frac{1}{2}(\mathrm{d}M/\mathrm{d}t)\,v^2 = \frac{1}{2}\rho v^3 h$, and the other half is dissipated. This accounts for the difference between (1) and (5).

The method of analysis using a frame of reference moving with the rim can be used to demonstrate that a change of liquid viscosity will not affect the rim velocity. With the rim fixed, it is instructive to calculate the Reynolds number for the flowing film, defined as $\rho v h/\mu$, μ being the liquid viscosity. In the present experiments, the orders of magnitude were: $\rho \approx 1000$ kg/m³, $v \approx 10$ m/s, $h \approx 0.5\ \mu\mathrm{m}$, $2 \leqslant \mu \leqslant 200$ mPa s; these figures give $2.5 \geqslant Re \geqslant 0.025$. It follows that viscous forces are substantial; presumably they are adequate to dissipate the kinetic energy of the elements of film entering the rim.

3.4. *Motion of the moving rim: non-spherical path*

The 'centrifugal force' on the rim will tend to make it follow a non-spherical path, causing the rim to move out to a larger radius than the radius of the original spherical soap film. Assuming that the rim *does* move in a spherical path, it is helpful to compare the surface tension forces on the rim, 2γ per unit length of rim, with the 'centrifugal force' mv^2/a, m being the mass of the rim per unit length, and a the radius of the spherical film: using (5) to get v, the two forces have the same magnitude when the rim has moved halfway round the sphere. Hence it is to be expected that the rim will move out to radii larger than a. The fact that in the experiments the rim appeared to move closely round the contour of the spherical film is probably due to droplet shedding from the growing rim. Droplet shedding would reduce the mass of the rim and hence reduce the magnitude of the above-mentioned 'centrifugal force'. As noted in §3.2, droplet shedding may not affect the energy balance leading to (5).

4. Results and discussion

4.1. *Film thickness and drainage time*

The initial film thickness of the spherical bubbles, formed by the method of §2.1, was in the range 0.2–$0.9\ \mu\mathrm{m}$; there was considerable variation in the thickness of the film formed on the top tube (figure 4) and the ultimate film thickness depended on the radius of the sphere into which the film was formed. As noted in §2, the film drained, owing to gravity, the liquid accumulating at the top of the bottom tube. Table 2 shows values of the initial thickness h, and the time t_c at which the film reached its critical thickness h_c when the bubble burst naturally.

Solution and symbol		Initial dia. (mm)	Initial thickness $h(\mu m)$	Critical thickness $h_c(\mu m)$	Stability time $t_c(s)$
A	○	70	0.51 ± 0.07	0.09 ± 0.02	6 ± 3
A	□	70	0.268 ± 0.02	0.07 ± 0.03	4 ± 3
A	▽	40	0.72 ± 0.2	0.07 ± 0.02	12 ± 2
B	△	80	0.29 ± 0.02	0.05 ± 0.04	7 ± 2
B	×	40	0.47 ± 0.16	0.06 ± 0.03	13 ± 3
C	●	80	0.324 ± 0.06	0.05 ± 0.01	9 ± 2
D	■	80	0.41 ± 0.01	0.06 ± 0.02	10 ± 2
D	▲	40	0.72 ± 0.18	0.07 ± 0.02	13 ± 2
E	▼	40	0.56 ± 0.03	0.08 ± 0.02	18 ± 6
E	⊖	60	0.32 ± 0.2	0.07 ± 0.02	14 ± 5

TABLE 2. Average film thicknesses for spherical bubbles, obtained from the electrical conductivity between tubes, figure 4: t_c is the time for drainage from h to h_c

These values of h_c are in reasonable agreement with the experimental data of Sheludko (1967) who reported values in the range $0.03 < h_c < 0.07\ \mu m$, quite similar to the results in table 2. The theoretical prediction of Patzer & Homsy (1975), $h_c \approx 0.9\ \mu m$ is much larger than these experimental findings.

Table 2 shows that the drainage time t_c increases with liquid viscosity, as would be expected.

The drainage process must be complex and it is not clear what is the mechanism by which the film finally ruptures spontaneously: these are unsolved problems. Order-of-magnitude estimates of film drainage rate were made by assuming (i) a parabolic velocity profile in the liquid film and (ii) the boundary condition of zero velocity at both surfaces of the liquid film on the supposition that the surfactant causes the interfaces to be rigid; it is by no means certain that this assumption will be justified in practice. These order-of-magnitude estimates gave values of t_c similar to the measured values in table 2.

4.2. *Rim velocity*

Results from the two methods of estimating rim velocity, described in §2.3, are shown in figure 6, together with the theoretical result (5). The theory is in good agreement with experiment. The error bars show the ranges of velocities from the frame-by-frame analysis, which gives higher velocities than the values from the overall rupture time. The reason for this difference may be as follows. The velocity obtained from the overall rupture time is based on the supposition that the rim travels a distance πa between puncture and final implosion, a being the radius of the spherical film. In fact the distance will be greater, owing to the centrifugal effect noted in §3.5, so the method will underestimate the velocity. The frame-by-frame method is based on the distance travelled from one frame to the next, thus giving a more realistic estimate of rim velocity.

Mysels & Vijayendran (1973) reported measurements of rim velocity for a flat soap film of thickness h up to $1\ \mu m$, using laser beams to measure the film thickness and rim velocity. In the range $0.1 < h < 1\ \mu m$, good agreement with (5) was obtained. For thinner films, windage was significant because of the higher rim velocities; consequently, the measured velocities, for $h < 0.1\ \mu m$, were below the prediction of (5).
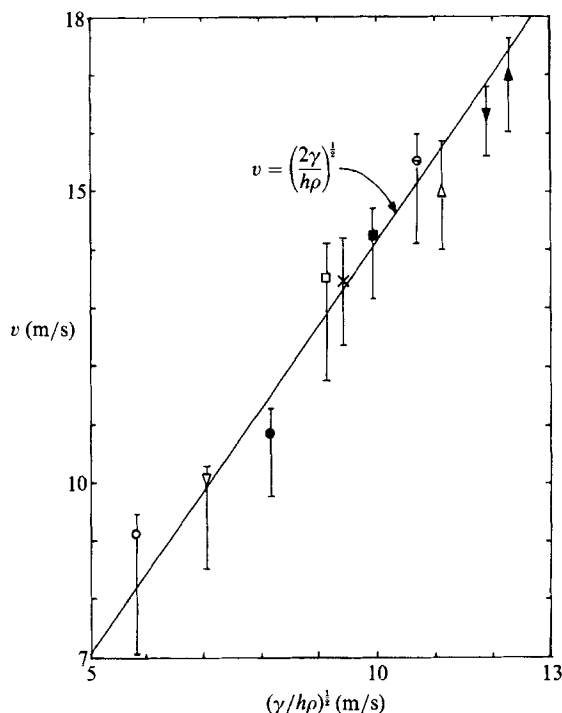
FIGURE 6. Relation between rim velocity and relevant variables: film thickness h: surface tension γ; liquid density ρ. The points (key in table 2) give the average velocity from the total rupture time. The error bars give the range of velocities from observations of single frames. The line shows equation (5).

It is notable, from figure 6, that the rim velocity is independent of liquid viscosity: the glycerol films have the same velocity as the aqueous solutions, although the viscosity of the glycerol is up to 130 times higher. Viscous forces evidently do not affect the rate at which the rim picks up elements of the very thin liquid film.

4.3. *Mean droplet size and size distribution*

The method of §2.5 gave the number of droplets generated by droplet shedding from the rim and from the final implosion: typically 4000–80000 droplets were generated. Table 3 shows the number of droplets, the mean size and the standard deviation of size, for a variety of conditions. The product (number of droplets) $\times \frac{1}{6}\pi d^3$, where d is the mean droplet diameter, gave the total liquid volume, which was consistent with the estimated liquid volume of the original spherical bubble, using the film thickness measured by the electrical conductivity method, §2.2.

However, the surface area of the droplets, crudely estimated from (number of droplets) $\times \pi d^2$ is only about 3–6% of the surface area of the film forming the original bubble. Thus the surface energy of the droplets is only a small proportion of the original surface energy of the film as found by previous workers (Ranz 1959; Blanchard 1963). This is plausible: comparing (1) and (5) shows that only half the surface energy of the film is converted into kinetic energy of the moving rim. Implosion of the rim must cause further dissipation of energy. Moreover the droplets have their own kinetic energy, likely to be comparable with the kinetic energy of the rim, for the droplets shed from the rim must leave with a velocity comparable with that of the rim.

Solution	Initial sphere dia. (mm)	Number of drops	Drop diameter (μm)	$100 \times \dfrac{\text{drop area}}{\text{film area}}$ (%)
A	80	$80\,000 \pm 20\,000$	50 ± 30	3.2 to 4.0
B	40	$13\,000 \pm 2000$	80 ± 30	5.72 to 6.0
C	60	$27\,000 \pm 3000$	70 ± 40	3.67 to 4.0
D	20	4000 ± 2000	80 ± 30	6.4 to 9.2
E	30	680 ± 300	320 ± 150	1.9 to 2.6

TABLE 3. Drop formation from spherical liquid films: number, mean diameter and its standard deviation; percentage of original film area as drops

Qualitative observations indicated that the mean droplet size was influenced by two factors namely: (i) the initial thickness h of the spherical film, the droplet size increasing with h; (ii) the liquid viscosity μ, the droplet size increasing with μ.

5. Conclusions

For a 'soap bubble' – formed from water or glycerol with dissolved surfactant – the liquid film thickness is typically 0.3–0.9 μm when first formed.

If such a film is ruptured at a point, the hole in the film enlarges rapidly, with a constant velocity of order 10 m/s: this is the velocity of the rim bounding the hole; the moving liquid gathers up the liquid from the film in its path. The velocity of the rim is well predicted by simple theory using either (i) a balance between the surface tension forces and the momentum of the rim or (ii) an energy balance, which gives the same expression for the rim velocity as method (i); the energy balance is instructive in demonstrating that there is continuous energy dissipation as the moving rim collides with elements of the stationary film.

Droplets are generated from the spherical film by two mechanisms namely: (i) break-up of the rim as it moves round the surface of the original sphere; (ii) 'implosion' of the liquid rim as its remaining elements converge on a point diametrically opposite to the point of the original puncture. Measurements show that a typical spherical film 60 mm diameter 0.4 μm thick gives, by the two mechanisms, a total of about 27000 droplets of mean diameter 70 μm. These droplets have a surface energy only a few per cent (3–6%) of the original surface energy of the spherical film.

The unpunctured spherical film drains, owing to gravity, eventually becoming naturally unstable when its thickness is of order 0.07 μm. The mechanisms of drainage and of rim instability deserve further study.

REFERENCES

BLANCHARD, D. C. 1963 Electrification of the atmosphere. In *Progress in Oceanography*, vol. 1 (ed. M. Sears), p. 71. Pergamon.

CULICK, F. E. C. 1960 Comments on a ruptured soap film. *J. Appl. Phys.* **31**, 1128.

DOMBROWSKI, N. & FRASER, R. P. 1954 A photographic investigation into the disintegration of liquid sheets. *Phil. Trans. R. Soc. Lond.* A **247**, 101.

MAJUMDAR, S. R. & MICHAEL, D. H. 1976 The equilibrium and stability of two-dimensional pendent drops. *Proc. R. Soc. Lond.* A **351**, 89.

MYSELS, K. J. & VIJAYENDRAN, B. R. 1973 Film bursting V. The effect of various atmospheres and the anomaly of Newton black films. *J. Phys. Chem.* **77**, 1692.

PANDIT, A. B., PHILIP, J. & DAVIDSON, J. F. 1987 The generation of small bubbles in liquids. In *Intl. Chem. Reac. Engineering Conf., II, Pune, India*, p. 72.

PATZER, J. F. & HOMSY, G. M. 1975 Hydrodynamic stability of thin spherically concentric fluid shells. *J. Colloid Interface Sci.* **51**, 499.

RANZ, W. E. 1959 Some experiments on the dynamics of liquid films. *J. Appl. Phys.* **30**, 1950.

RAYLEIGH, LORD 1891 Some applications of photography. *Nature* **44**, 249. (Also *Scientific Papers* vol. 3, 1898, p. 441.)

RAYLEIGH, LORD 1945 *Theory of Sound*, vol II, p. 360. Dover.

RUTLAND, D. F. & JAMESON, G. J. 1971 A non-linear effect in the capillary instability of liquid jets. *J. Fluid Mech.* **46**, 267.

SHELUDKO, A. 1967 Thin liquid films. In *Advances in Colloid and Interface Science*, vol. 1, p. 391. Elsevier.

TAYLOR, G. I. 1960 Formation of thin flat sheets of water. *Proc. R. Soc. Lond.* A, **259**, 1. (Also *Scientific Papers of G. I. Taylor*, Vol. IV, 1971, p. 378.)

TAYLOR, G. I. & MICHAEL, D. H. 1973 On making holes in a sheet of fluid. *J. Fluid Mech.* **58**, 625.